

Critical Buckling Load Analysis Of A Composite At The Base Of On A Double-Walled Carbon Nanotube Reinforcement And An Elastic Polymer Matrix

Belmahi Samir¹, Boulesnane Nedjm Eddine¹, Zidour Mohamed¹

¹*Institute of sciences and Technology, University Centre of Maghnia, Algeria.*

¹*University of Tiaret, Algeria, Department of Civil Engineering.*

¹*University of Tiaret, Algeria, Department of Civil Engineering, Geomatics and sustainable development laboratory (LGéo2D)*

The quality of new materials, notably the composites is judged by knowledge of its reactions and its resistances to different mechanical behavior under the effect of different types of loading. The current paper presents the study of buckling under the effect of a $q(x)$ loading of a nanocomposite composed of a reinforcement of double-walled carbon nanotube (DWCNT) and an elastic matrix a polyethylene type polymer. The beam model chosen for the calculation is that of Euler-bernouli and the elastic model is that of Winkler. Pasternak's model was subsequently concluded. The critical buckling load (P_{cr}) of this composite was determined using the non-local elasticity theory which takes into account the small scale effect (e_0a) and the effect of the elastic Van der Waals forces between the tubes of CNT. Several parameters on the effect of the critical buckling load were considered and discussed such as, the chirality of CNT and their geometric ratio (L/D), the nonlocal effect (e_0a), the mode number (N) and the stiffness of the elastic matrix. The results showed the importance of these parameters and their significant impact on the critical buckling load. it increases when the geometric ratio (L/d) and the small-scale coefficient (e_0a) decrease and when the mode number (N) and chirality number (n) increase. Moreover, it turns out that the application of the nonlocal elasticity theory model is important and necessary for high mode numbers and small-scale coefficient (e_0a) and for short nanotubes. Thus, the incorporation of CNTs into an elastic polymer matrix makes it possible to obtain a very rigid nanocomposite material with an exceptional critical buckling load. The results also highlight the importance of taking into account the different parameters linked to the material studied as well as other external effects.

Keywords: Buckling, Carbon Nanotubes, Composite, Reinforcement, Euler-Bernoulli. Nonlocal theory.

1. Introduction

Composites based on carbon nanotubes constitute today have constituted a fundamental element studies in general in materials sciences and in particular in nanotechnologies (Ahmadi et al., 2016, Belmahi et al., 2019). They have sparked numerous research activities, closely linked to their extraordinary physico-mechanical (strength-to-weight ratio, specific stiffness), chemical and thermal properties (Keivan 2014, Omar, 2019, Xuan-Bach et al., 2023, Haoting et al., 2024). The carbon nanotubes represents an allotropic form of carbon distinct from diamond and graphite (Kaushik et al., 2015) and has only a single layer of graphene coiled on itself (Peter 1999). CNTs are ultimate reinforcing agents, called nanofibers, in different matrix materials for the development of a new class of extremely strong and ultra-lightweight nanocomposites (Dinesh et al., 2016, Belmahi et al., 2019, Haoting et al., 2024). Nanocomposites are materials presenting a nanometric structure at a scale between 1 and 100 nm (Henriette et al., 2009, Ashton 2013, Charles 2014). They have the capacity to improve the macroscopic properties of products as well as the mechanical properties, without compromising the ductility of the material (Bakis et al., 2002, Charles 2013, Sachse et al., 2013,). They are considered homogeneous at the macroscopic level and heterogeneous at the microscopic level (Belmahi et al., 2019). Their use is based on knowledge, at different scales, of their behavior and characteristics taking into account the different factors that intervene (Hurang et al., 2010, Shehata et al., 2011). In a composite, the carbon nanotube represents the reinforcement which is responsible for overall stability, particularly mechanical performance. It increases the rigidity which implies the increase in the Young's modulus and the breaking stress of the nanocomposite. It is associated with a filler or a matrix which can in the general case be a polymer or an organic material which ensures cohesion (Hurang et al., 2010, Charles 2013, Shokuhfar et al., 2013, Kaushik et al., 2015, Haoting et al., 2024). Nano-composites based on carbon nanotubes are currently of interest to several fields in mechanics, in construction such as a recess, in the aerospace industry and aeronautics (Mrazova, 2013, Xuan-Bach et al., 2023, Basati et al., 2024, Emrah et al., 2024).

Several questions have been developed on this material, in particular free and forced vibration, among which we cite some work : on the linear and nonlinear vibration analysis by the use and application of different theories: by Timoshenko beam theory (Ansari et al., 2013), by nonlocal Euler-Bernoulli beam theory (Necla et al., 2016, Rakrak 2016), by variational iteration method (Hajnayeb et al., 2015, Ahmadi et al., 2016) and other works on vibration: (Gafour, et al., 2013, Danilo et al., 2015, Ramezani, et al., 2015, Soltani et al., 2015, Rakrak et al., 2016, Tuan et al., 2017, Dihaj et al., 2018, Hamidi et al., 2018). Carbon nanotubes (CNTs) are susceptible to buckling or structural instability due to their long and hollow tubular structures (Iijima et al., 1996, Motevall et al., 2012). This can significantly influence their performance as structural or functional elements in CNT-based nanocomposites (Ball, 2001, Qian et al., 2002, Zhang.y et al., 2007). The buckling present a deformation process in which a structure affected with to high stress dergoes a sudden change in morphological state at a critical load (Chemi et al., 2018). According to the authors

(Mahmood et al., 2004, Wang et al., 2006, Hiroyuki, 2011), for small loads, the beam is compressed in the axial direction while maintaining its linear shape, and the strain energy is proportional to the square of the axial displacement. However, beyond a certain critical load, it suddenly bends in an arc and the relationship between strain energy and displacements deviates considerably from the square law. Besides axial compression, bending and torsion give rise to buckling behaviors of elastic beams, where buckling patterns strongly depend on geometric and material parameters. In this context, several works on the buckling of carbon nanotubes have been carried out, we quote: the Buckling under Axial Compression: (Zhang et al., 2007) with Molecular Dynamics (MD) simulations, they have been observed that a SWCNT with an aspect ratio of 6 remains in its cylindrical shell configuration but becomes shorter under axial compression prior to buckling. The Buckling under bending moment and axial compression: (Chang et al., 2005) proved that SWNTs possess extraordinary structural flexibility, they can undergo stretching and compression and they return to the in the initial state. More recent studies on composites based on carbon nanotubes such as: the buckling of stiffened panels made of carbon and glass fiber reinforced composites by Haoting et al., 2024, buckling of a composite beam reinforced with carbon fibers /fibers under mechanical and thermal loads by Xuan-Bach et al.2023; Basati et al., 2024 and under compressive load by PatrykRozylo, 2023 and Kuba et al., 2023. Buckling of a CNT-reinforced polymer composite beam using experimental and analytical methods by Emrah et al., 2024.

The study that we will present in this work has the objective and particularity of analyzing the critical buckling load of a composite composed of a double-walled carbon nanotube (DWCNT) reinforcement incorporated in a polymer matrix which represents the elastic medium according to the Winkler model. Therefore, the Euler-Bernoulli calculation model and the theory of nonlocal elasticity are used. The carbon nanotube considered in this work is of the double wall type (DWCNTs).

2. Calculation of critical buckling load

2.1 Application of Nonlocal Theory

In nonlocal elasticity theory the stress at a reference point (x) is considered as a function of the strain field estimated at each point in the body. This observation is consistent with the atomic model and experimental observations on photon dispersion. Furthermore, when the effect of stresses at points other than (x) is neglected, the nonlocal theory of elasticity conforms to the classical (local) theory of elasticity by settingsmall scale effect ($e_0 a = 0$). Therefore, the nonlocal theory provides a more precise description of material behavior compared to the classical (local) theory of elasticity. The basic equations for a nonlocal, linear, homogeneous and isotropic elastic solid, not subject to an external force are given by (Belmahi et al., 2018)

$$\begin{cases} \sigma_{ij,j} = 0 \\ \sigma_{ij}(x) = \int \alpha(|x - x'|, \tau) C_{ijkl} \varepsilon_{kl}(x') dV(x'), \quad \forall x \in V \\ \varepsilon_{ij} = \frac{1}{2} (u_{i,j} + u_{j,i}) \end{cases} \quad (1)$$

Where:

C_{ijkl} is the classical macroscopic stress tensor at point x' ,

σ_{ij} and ε_{ij} are stress and strain tensors respectively,

$\alpha(|x - x'|, \tau = e_0 a/l)$: is the kernel function

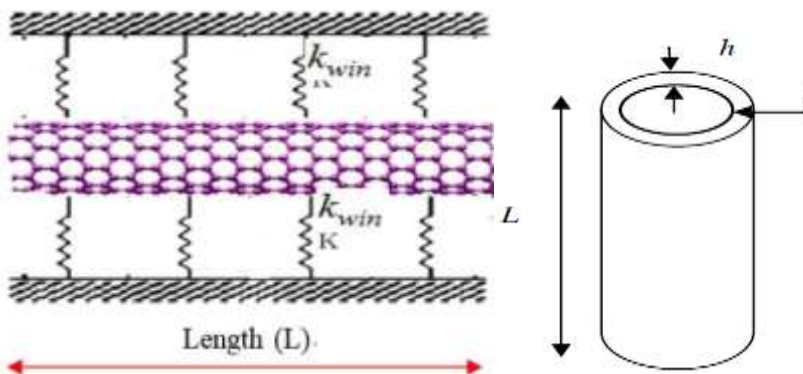
2.2 Calculation

Consider a nanocomposite represented by nanobeam of length L , of uniform section A and of constant Young's modulus E .

the nanobeam is composed of a carbon nanotube reinforcement integrated in an elastic medium of the Winkler type which represents the matrix (figure 1).

The variables x and w represent respectively the axial coordinate and the transverse displacement.

Figure 1 Geometries and arrangement of a CNT integrated in an Winkler elastic medium (Belmahi et al., 2019).



The following terms will be used in the development below:

k_{win} : rigidity winkler (depending on the type of polymer matrix).

λ : Buckling slenderness ratio.

$e_0 a$: small scale effect.

E : Young's modulus.

I : Moment of inertia.

t : Carbon nanotube layer thickness.

d_1, d_2 : are respectively the radiuses of the inner and outer tubes.

M : bending moment.

V : shear force.

q : is the distributed load on the nanobeam

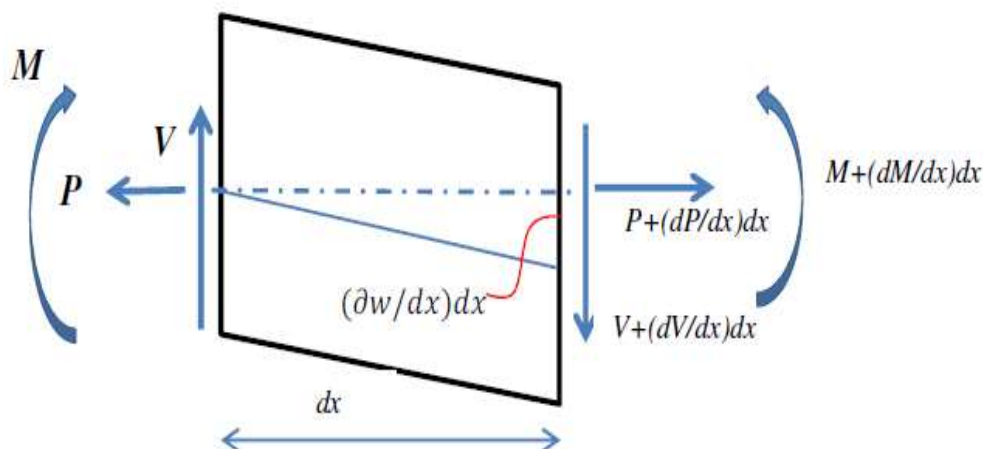
The non-local constitutive relation approximated to a one-dimensional form and the deformation ε for the Euler-Bernoulli model are given by (Belmahi et al., 2019):

$$\sigma(x) - (e_0 a)^2 \frac{\partial^2 \sigma(x)}{\partial x^2} = E \varepsilon(x) \quad (2)$$

$$\varepsilon(x) = -y \frac{d^2 w(x)}{dx^2} \quad (3)$$

Consider a homogeneous beam of constant section (A). In the case of the Euler-Bernoulli beam model, the transverse vibration motion is described as follows (figure 2):

Figure 2 Elementary representation of the Euler Bernoulli beam.



The force and moment balance equations can be easily provided from the free body diagram of an infinitesimal element of a beam structure subjected to an axial load P [1].

$$\frac{dV}{dx} = -q(x) + k_{\text{win}} w(x) \quad (4)$$

$$\frac{dM}{dx} = -P \frac{dw}{dx} + V \quad (5)$$

D'où

$$\frac{d^2 M}{dx^2} = -P \frac{d^2 w}{dx^2} + \frac{dV}{dx} \quad (6)$$

Let us substitute equation (4) into (6):

$$\frac{d^2 M}{d^2 x} = -P \frac{d^2 w}{d^2 x} - q(x) + k_{win} w(x) \quad (7)$$

The resulting bending moment in a beam section is given as follows:

$$M = \int_A^1 y \sigma dA \quad (8)$$

From relations (2), (3) and (8), the bending moment M for the nonlocal model can be expressed by:

$$M = (e_0 a^2) \frac{\partial^2 M}{\partial^2 x} - E \int_A^1 y^2 dA \frac{d^2 w}{d^2 x} \quad (9)$$

Knowing that the moment of inertia

$$I = \int_A^1 y^2 dA \quad (10)$$

Equation (9) become:

$$[1 - (e_0 a^2) \frac{d^2}{d^2 x}] M = -EI \frac{d^2 w}{d^2 x} \quad (11)$$

Substituting equation (7) into equation (12) and deriving gives the following equation (12):

$$\frac{d^2 M}{d^2 x} = -EI \frac{d^4 w}{d^4 x} + (e_0 a^2) \left[-P \frac{d^4 w}{d^4 x} - \frac{d^2 q(x)}{d^2 x} + k_{win} \frac{d^2 w}{d^2 x}(x) \right] \quad (12)$$

Substituting equation (7) again into equation (12), we obtain:

$$-P \frac{d^2 w}{d^2 x} - q(x) + k_{win} w(x) = -EI \frac{d^4 w}{d^4 x} + (e_0 a^2) \left[-P \frac{d^4 w}{d^4 x} - \frac{d^2 q(x)}{d^2 x} + k_{win} \frac{d^2 w}{d^2 x}(x) \right] \quad (13)$$

By simplification

$$EI \frac{d^4 w}{d^4 x} + (1 - (e_0 a^2) \frac{d^2}{d^2 x}) \left[-P \frac{d^2 w}{d^2 x} - q(x) + k_{win} w(x) \right] = 0 \quad (14)$$

The Van der Waals pressure should be a linear function of the difference in deflections of the two layers adjacent to the point as follows:

$$q_{12} = ct(w_2 - w_1) \quad (15)$$

$$q_{21} = -\frac{d1}{d2} ct(w_2 - w_1) \quad (16)$$

Where, d1 and d2 are the radius of the inner and outer tubes respectively.

Substituting equation (15), then equation (16) into equation (14), we obtain the following system of equation (17):

$$\begin{cases} EI \frac{d^4 w_1}{dx^4} + (1 - (e0a^2) \frac{d^2}{dx^2}) [-P \frac{d^2 w_1}{dx^2} - ct(w_2 - w_1) + kwinw_1(x)] = 0 \\ EI \frac{d^4 w_2}{dx^4} + (1 - (e0a^2) \frac{d^2}{dx^2}) [-P \frac{d^2 w_2}{dx^2} + \frac{d1}{d2} ct(w_2 - w_1) + kwinw_2(x)] = 0 \end{cases} \quad (17)$$

Let us assume the following sinusoidal buckling functions as a solution to the previous system (17)

$$\begin{cases} w_1 = W1 \sin(\lambda x) \\ w_2 = W2 \sin(\lambda x) \end{cases} \quad (18)$$

After substituting equation (18) into equation (17) we obtain the following homogeneous system:

$$\begin{cases} [EI_1 \lambda^4 + (1 + e0a^2 \lambda^2)(ct + kwin + P\lambda^2)] W1 - [(1 + e0a^2 \lambda^2) ct] W2 = 0 \\ [-(1 + e0a^2 \lambda^2) \frac{d1}{d2} ct] W1 + [EI_2 \lambda^4 + (1 + e0a^2 \lambda^2)(\frac{d1}{d2} ct + kwin + P\lambda^2)] W2 = 0 \end{cases} \quad (19)$$

It is written in matrix form as follows:

$$\begin{bmatrix} k_{11} & k_{12} \\ k_{21} & k_{22} \end{bmatrix} \begin{pmatrix} W1 \\ W2 \end{pmatrix} = 0 \quad (20)$$

With :

$$\begin{cases} k_{11} = EI_1 \lambda^4 + (1 + e0a^2 \lambda^2)(ct + kwin + P\lambda^2) \\ k_{12} = (1 + e0a^2 \lambda^2) ct \\ k_{21} = (1 + e0a^2 \lambda^2) \frac{d1}{d2} ct \\ k_{22} = EI_2 \lambda^4 + (1 + e0a^2 \lambda^2)(\frac{d1}{d2} ct + kwin + P\lambda^2) \end{cases} \quad (21)$$

So the determinant:

$$[EI_1 \lambda^4 + (1 + e0a^2 \lambda^2)(ct + kwin + P\lambda^2)] * [EI_2 \lambda^4 + (1 + e0a^2 \lambda^2)(\frac{d1}{d2} ct + kwin + P\lambda^2)] - [-(1 + e0a^2 \lambda^2) ct] * [-(1 + e0a^2 \lambda^2) \frac{d1}{d2} ct] = 0 \quad (22)$$

And the solution will be as follows:

$$a_1 P^2 + b_1 P + c_1 = 0 \quad (23)$$

With:

$$\left\{ \begin{array}{l} a_1 = \lambda^4 + e0a^4\lambda^8 + 2e0a^2\lambda^6 \\ b_1 = 2e0a^4\lambda^6 k_{win} + EI_1\lambda^8 e0a^2 + 2\lambda^2 k_{win} + 4\lambda^4 e0a^2 k_{win} + e0a^4\lambda^6 \frac{d1}{d2} ct \\ \quad + 2cte0a^2\lambda^4 + EI_1\lambda^6 + \lambda^6 EI_2 + e0a^2\lambda^8 EI_2 + ct\lambda^2 + \lambda^2 \frac{d1}{d2} ct + e0a^4\lambda^6 ct \\ \quad + 2\lambda^4 e0a^2 \frac{d1}{d2} ct \\ c_1 = e0a^4\lambda^4 k_{win}^2 + k_{win} EI_2\lambda^4 + k_{win} \frac{d1}{d2} ct + e0a^2\lambda^6 ct EI_2 + 2e0a^2\lambda^2 k_{win}^2 \\ \quad + ct EI_2\lambda^4 + E^2 I_1\lambda^8 I_2 + e0a^2\lambda^6 k_{win} EI_2 + EI_1\lambda^4 k_{win} + e0a^4\lambda^4 ct k_{win} + k_{win}^2 \\ \quad + 2cte0a^2\lambda^2 k_{win} + e0a^4\lambda^4 k_{win} \frac{d1}{d2} ct + ct k_{win} + EI_1\lambda^6 e0a^2 k_{win} \\ \quad + 2k_{win} e0a^2\lambda^2 \frac{d1}{d2} ct + EI_1\lambda^4 \frac{d1}{d2} ct + EI_1\lambda^6 e0a^2 \frac{d1}{d2} ct \end{array} \right. \quad (24)$$

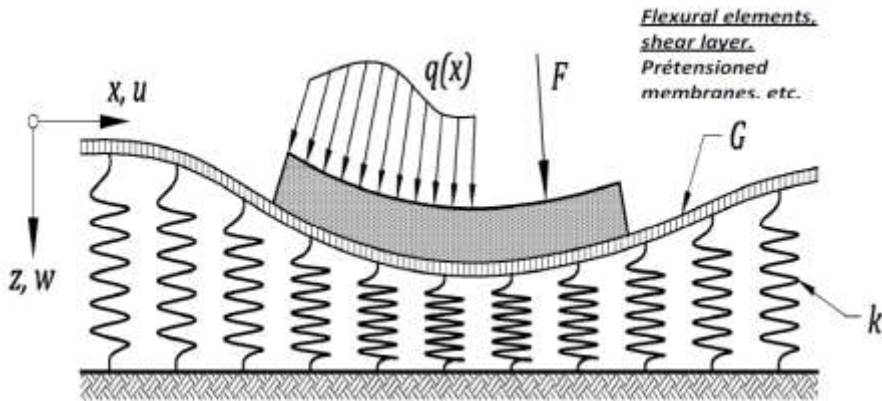
So, the final equation that solves system (24) and will give us the critical buckling load (P_{cr}) of DWCNT-nanocomposite in which the effect of the Winkler elastic medium together with the different parameters were considered is the following:

$$P_{cr1} = \frac{-b_1 \pm \sqrt{b_1^2 - 4a_1 c_1}}{2a_1} \quad (25)$$

2.3 The case of Pasternak elastic model

In Pasternak model the interaction between the different layers of an elastic medium was represented by a layer made up of incompressible vertical elements which only deform by transverse shear of Pasternak rigidity k_p and which will be connected to the ends of winkler springs. This is the Winkler-Pasternak model.

Figure 3 Beam on two-parameter elastic foundation (Winkler-Pasternak) (Dobromir, 2012)



The pressure-deflection relationship according to the Pasternak model is given by (Dobromir, 2012):

$$f(x) = k_{win} w - k_P w \frac{\partial^2 w}{\partial x^2} \quad (26)$$

Replacing the Winkler elastic medium model given in equation (4) by the Pasternak model given in formula (26) and following the same development above we find the new critical buckling load as a function of the Pasternak elastic medium which takes into consideration the shear between the layers of the elastic medium:

$$P_{cr2} = \frac{-b_2 \pm \sqrt{b_2^2 - 4a_2c_2}}{2a_2} \quad (27)$$

The coefficients of the real numbers are:

$$\left\{ \begin{array}{l}
 \mathbf{a}_2 = e0a^2 2\lambda^6 + \lambda^4 + e0a^4 \lambda^8 \\
 \mathbf{b}_2 = ct\lambda^2 + \lambda^6 EI_2 + 2\lambda^4 kp + \frac{2d1\lambda^4 e0a^2}{d2} ct + ct\lambda^6 e0a^4 + 4e0a^2 \lambda^4 k_{win} \\
 + 2e0a^4 \lambda^6 k_{win} + e0a^2 \lambda^8 EI_2 + \frac{d1\lambda^6 e0a^4}{d2} ct + 4\lambda^6 e0a^2 kp + 2ct\lambda^4 e0a^2 \\
 + 2\lambda^2 k_{win} + 2e0a^4 \lambda^8 kp + \frac{d1\lambda^2}{d2} ct + \lambda^8 EI_1 e0a^2 + \lambda^6 EI_1 \\
 \mathbf{c}_2 = 2\lambda^6 e0a^2 kp^2 + \lambda^8 e0a^4 kp^2 + 2\lambda^2 e0a^2 k_{win}^2 + 2\lambda^2 k_{win} kp \\
 + ct k_{win} + \frac{d1\lambda^4 EI_1}{d2} ct + \lambda^6 EI_1 e0a^2 k_{win} + \lambda^6 EI_1 kp + \lambda^8 EI_1 e0a^2 kp \\
 + ct\lambda^4 EI_2 + ct kp\lambda^2 + k_{win} \lambda^4 EI_2 + 4\lambda^4 k_{win} e0a^2 kp + kp\lambda^6 EI_2 \\
 + 2\lambda^6 k_{win} e0a^4 kp + 2\lambda^2 e0a^2 k_{win} ct + 2\lambda^4 e0a^2 kp ct + \frac{d1k_{win}}{d2} ct + \frac{2d1k_{win}\lambda^2 e0a^2}{d2} ct \\
 + \frac{\lambda^2 d1kp}{d2} ct + \frac{2d1kp\lambda^4 e0a^2}{d2} ct + \lambda^6 e0a^2 EI_2 ct + \lambda^4 e0a^4 k_{win} ct + \lambda^6 e0a^4 kp ct \\
 + \lambda^6 EI_2 e0a^2 k_{win} + \frac{d1k_{win}\lambda^4 e0a^4}{d2} ct + \lambda^8 EI_2 e0a^2 kp + \frac{d1kp\lambda^6 e0a^4}{d2} ct \\
 + \lambda^4 e0a^4 k_{win}^2 + EI_1^2 EI_2 \lambda^8 + \frac{d1EI_1\lambda^6 e0a^2}{d2} + \lambda^4 EI_1 k_{win}
 \end{array} \right. \quad (28)$$

Therefore:

$$\left\{ \begin{array}{l}
 d1 = \frac{\sqrt{3}}{\pi} a_{cc} \sqrt{(n^2 + m^2 + nm)} \\
 d2 = d1 + 2h
 \end{array} \right. \quad (29)$$

$$\left\{ \begin{array}{l}
 I1 = \frac{(d1+t)^4 - (d1-t)^4}{64} \pi \\
 I2 = \frac{(d2+t)^4 - (d2-t)^4}{64} \pi
 \end{array} \right. \quad (30)$$

2.4 Calculation Data

The nanocomposite is composed of a double-walled zigzag-like carbon nanotube reinforcement (DWCNT) with an effective thickness equal to $t = 0.285$ nm, the density $\rho = 2.3$ g/cm³, the distance between the layers $h = 0.34$ nm, the Poisson's ratio $\nu = 0.19$.

For the rigidity of the k_{win} elastic support, we have chosen a polyethylene type polymer; its value is $k_{win} = 0.9$ GPa.

The Young's modulus des (DWCNT) values used in this calculation were calculated by Bao et al., 2004, table 1.

Table 1 Young's modulus values of DWCNT for zigzag-like.

Hamada indices (n,m)	Young's modulus (DWNT) (GPa) Bao et al., 2004.
(14,0)	939.032
(17,0)	938.553
(21,0)	936.936
(24,0)	934.201
(28,0)	932.626
(31,0)	932.598
(35,0)	933.061

3. Results

The results discussed below will show how the different parameters of geometric ratio (L/D), small-scale coefficient (e_0a) and mode number (N) will affect the critical buckling load on a DWNTC integrated in an elastic matrix.

Table 2 Results of critical buckling load according to different parameters (Only maximum and minimum values).

N	2				6			
e_0a	0		2		0		2	
L/D	10	40	10	40	10	40	10	40
(14,0)	59.84	-111.96	36.90	-112.05	619.38	23.04	111.66	14.68
(17,0)	65.78	-143.98	44.07	-144.06	696.88	23.38	153.32	15.72
(21,0)	73.15	-192.90	53.11	-192.97	799.76	23.05	218.93	16.23
(24,0)	78.15	-234.28	59.33	-234.35	875.50	22.19	274.63	15.93
(28,0)	84.53	-295.68	67.18	-295.74	978.16	20.49	357.45	14.86
(31,0)	89.11	-346.41	72.73	-346.47	1056.35	18.81	425.30	13.58
(35,0)	94.84	-420.29	79.66	-420.35	1161.30	16.00	522.07	11.23

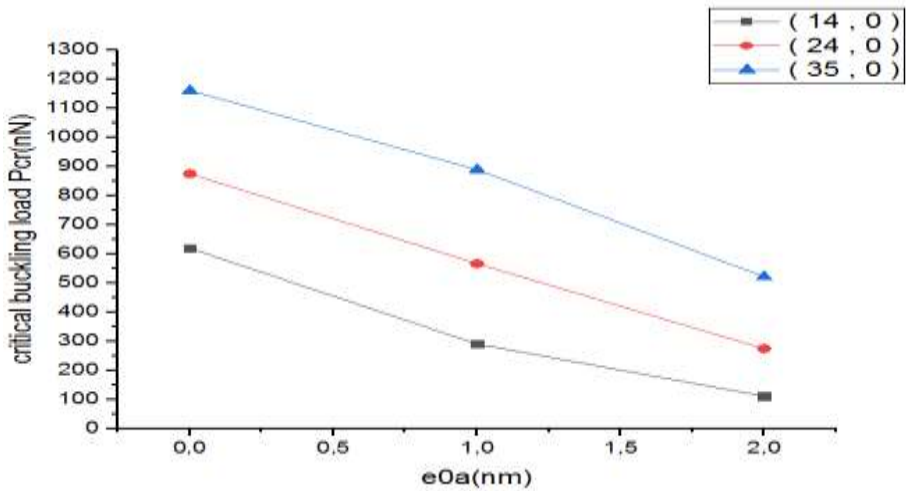
Table 3 Results of the critical buckling load as a function of the rigidity of the elastic matrix for chirality (14, 0) ($N=6$; $L/D=10$)

e_0a	$k_{win}=0$	$k_{win}=0,9$	$k_p=0,321$
0	650.66	619.38	602.24

1	398.52	395.01	390.33
2	113.32	111.66	101.26

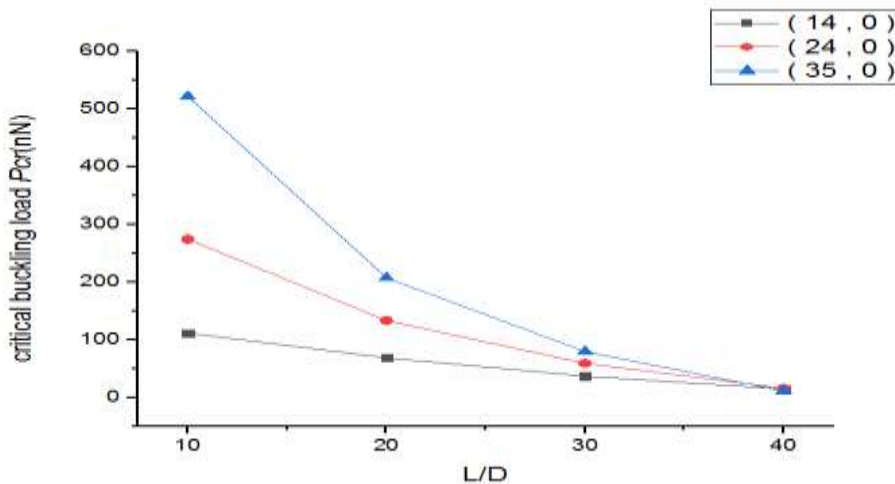
The results obtained from Table 2 and 3 are based on the theory of non-local elasticity and also on the integration of the Euler Bernouli beam model in the calculation.

Figure 4 Variation the critical buckling load (Pcr) and the small scale coefficient (e0a) of DWCNT L/D = 10 and N = 6) .



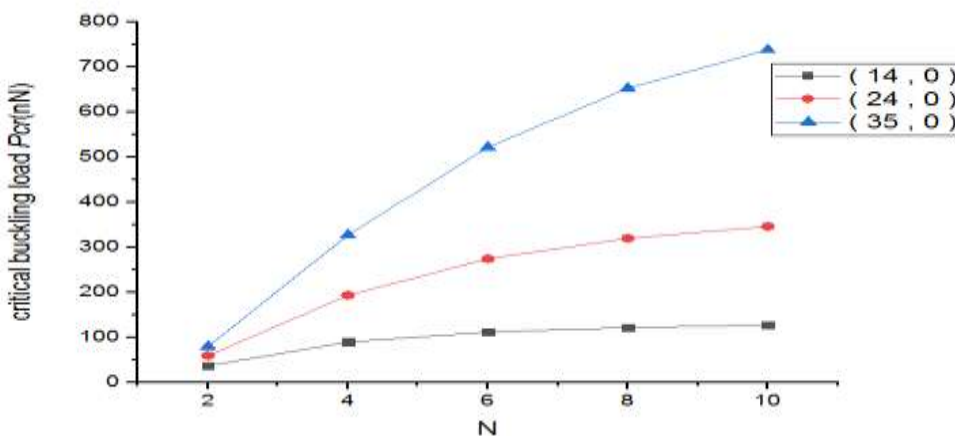
In figure 4, we see that the critical buckling load is smaller when the small scale coefficient taken into account in the calculation is high ($e0a = 2$). This explains the importance of using the non-local elasticity theory which gives a margin of safety in the calculation compared to the local elasticity theory. For example, in the case of a carbon nanotube with chirality (14. 0). It is see a difference in the critical buckling load of approximately 80% going from a small scale effect ($e0a = 0$ to 2). Also, we see that the critical buckling load increases with the increase in the hamada index (an increase of approximately 78% going from chirality ($n = 14$ to 35) according to the results of table 2 and figure 04.

Figure 5 Variation the critical buckling load (Pcr) in terms of the geometric ratio (L/D) of the DWCNT ($e0a = 2$ and $N = 6$).



The figure 5 represents the variation the critical buckling load (P_{cr}) in terms of the geometric ratio (L/D) of the DWCNT. It is seen that the critical buckling load increases when the geometric ratio of the reinforcement decreases (an increase of approximately 97% going from a geometric ratio ($L/D = 40$) to 10). This explains the importance of choosing the lowest possible geometric ratio (L/D) in order to have a high critical load and prevent the material from deforming perpendicular to the axis of the applied force when it is compressed in the lengthwise. This figure 5 also confirms the previous observation that the highest critical buckling load is relative to the highest hamada index.

Figure 6 Variation the critical buckling load (L_{cr}) in terms of the mode number (N) of the DWCNT ($e_0a = 2$ and $L/D = 10$).



The figure 6 represents the variation the critical buckling load (L_{cr}) in terms of the mode number. It is see that the critical buckling load increases both when the mode number N increases and when the chirality number increases in a remarkable way. For example, for the case of reinforcement with a chirality number ($n = 35$), the critical buckling load increases by approximately 70% going from $N = (2 \text{ to } 10)$ and we can have a difference in increase of 80% going from a number of chirality ($n = 14 \text{ to } 35$). Therefore the critical load is all the better for the modes and for the highest numbers of chirality. According to (Belmahi et al. 2018 & 2019) in the high modes the interactions between the atoms increase because of the short wavelength attributed to the small diameter of the carbon nanotube reinforcement and to the elastic matrix considered.

Figure 7 Variation of the critical buckling load (P_{cr}) as a function of the elastic medium ($L/D = 10$, $N=6$ and $eo_a = 2$)

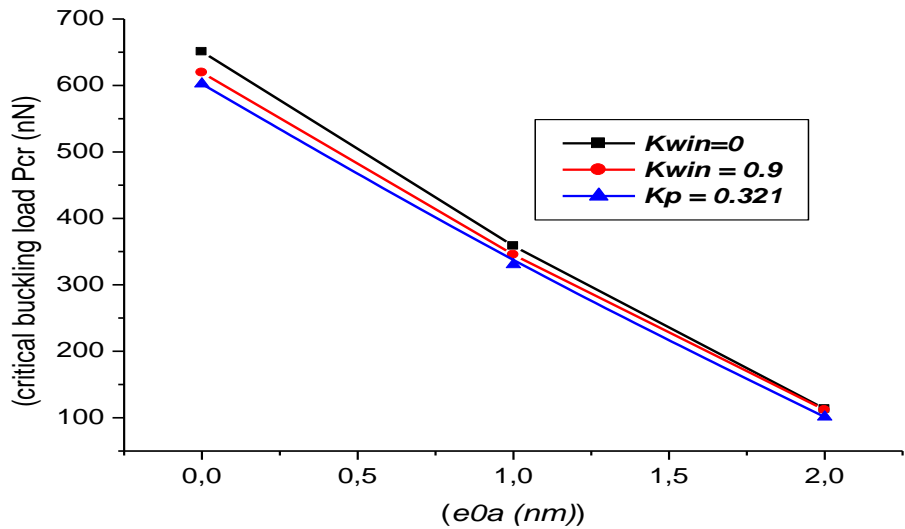


Figure 07 represents the variation of the critical buckling load as a function of the small-scale effect and for different types of elastic medium. it is noted and consistent with Figure 04 that for any type of elastic medium, the critical load decreases with the increase in the ratio at small scales ($e0a$) hence the importance of making a calculation with the non-local theory, also, a small difference is noted between the values of the critical load without elastic medium ($k_{win} = 0$) and with the presence of the elastic medium (polyethylene $k_{win} = 0.9$), this means that the assembly of these two materials does not It is not affected and remains perfect with characteristics close to the carbon nanotube. according to (Chemi et al., 2018), this small variation is attributed to the weak van der Waals forces between the internal and external tubes of the carbon nanotube. Indeed, according to (Belmahi et al., 2019) the matrix ensures the cohesion of the nanocomposite, while the carbon nanotube represents the reinforcement which

is responsible for these mechanical performances and overall stability. It is also noted that the critical buckling load calculated with the Pasternak model ($k_p = 0.321$) which is more generalized is less than in the case calculated with Winkler. therefore, the Pasternak calculation remains more secure.

4. Conclusion

In this paper, the study of the critical buckling load is important, such that in this work the latter was calculated for a carbon nanotube (DWCNT) represented by an Euler-Bernoulli nanobeam model and integrated in a Winkler type elastic matrix. Numerous parameters were taken into account including, the dimensional or geometric ratio (L/d), the small scale coefficient (e_0a) and the mode number (N) and the chirality number. The results have shown the dependence of the critical buckling load on the different parameters cited above. to have a high critical charge, you must have the lowest geometric ratio (L/d), the highest mode number (N) and chirality number and vice versa. thus the procedure with a small scale effect coefficient between 1 and 2 makes it possible to take into account the non-local effect and to have security in the calculation. Also, it can be concluded in the case of high rigidities than the non-local theory is necessary and the presence of a very rigid matrix reduces the critical buckling load and the Pasternak model is more secure in the calculation of this critical load than the Winkler model.

Disclosure Statement

No statement

References

1. Ahmadi A.A Asoor, "Valipour P. and Ghasemi S. E. (2016). Investigation on vibration of single-walled carbon nanotubes by variational iteration method, *ApplNanosci*, 6, 243–249. <https://doi.org/10.1007/s13204-015-0416-8>.
2. Belmahi samir, Mohammed Zidour and Mustapha Meradjah. (2019). Small-scale effect on the forced vibration of a nano beam embedded an elastic medium using nonlocal elasticity theory. *Advances in Aircraft and Spacecraft Science*, Vol. 6, No. 1 001-000. <https://doi.org/10.12989/aas.2019.6.1.001>.
3. Keivan Kiani. (2014). Vibration and instability of a single-walled carbon nanotube in a three-dimensional magnetic field. *Journal of Physics and Chemistry of Solids* 75, 15–22. <https://doi.org/10.1016/j.jpcs.2013.07.022>.
4. Omar A. Mohamed. Buckling Analysis of Hybrid Laminated Composite Beam Analytically and Numerically. (2019). *Iraqi academic scientific journal. Al-Rafidain Engineering Journal (AREJ)*. Vol. 24, No1, pp. 19-25.
5. Xuan-Bach Bui , Anh-Cao Nguyen , Ngoc-Duong Nguyen Tien-Tho Do, Trung-Kien Nguyen. (2023). Buckling analysis of laminated composite Thin-walled i-beam under mechanical and Thermal loads. *Vietnam Journal of Mechanics*, Vol. 45, No. 1, pp. 75–90. DOI: <https://doi.org/10.15625/0866-7136/17956>.
6. Haoting Han and Chensong Dong. (2024). Buckling Analysis for Carbon and Glass Fibre Reinforced Hybrid Composite Stiffened Panels. *J. Compos. Sci* V, 8, 34. <https://doi.org/10.3390/jcs8010034>.

7. Kaushik B.K. and Majumder M.K. (2015). Carbon Nanotube Based VLSI Interconnects analysis and design. Springer Briefs in Applied Sciences and Technology, 3 (2) 17-37. <https://link.springer.com/book/10.1007/978-81-322-2047-3>.
8. Peter J and Harris F. (1999). Carbon Nanotubes And Related Structures. New materials for the twenty-first century, Cambridge University Press. New York, NY100114211USA.https://personal.ems.psu.edu/~radovic/HarrisBook_Ch1.pdf.
9. Dinesh Kumar and Ashish Srivastava. (2016). Elastic properties of CNT- and graphene-reinforced nanocomposites using RVE. Steel and Composite Structures. 21, (5), 1085-1103.<https://doi.org/10.12989/scs.2016.21.5.1085>.
10. Henriette M.C and De Azeredo. (2009). Nanocomposites for food packaging applications. Food Research International 42, 1240–1253.<https://doi.org/10.1016/j.foodres.2009.03.019>.
11. Ashton Acton Q. (2011). Issues in hydrogen, fuel cell, electrochemical, and experimental technologies. Scholarly edition, Atlanta Georgia. https://books.google.dz/books?id=lQyQfw4C3GUC&printsec=frontcover&hl=fr&source=gbs_ge_summary_r&cad=0#v=onepage&q&f=false
12. Charles Chikwendu Okpala. (2014). The benefits and applications of nanocomposites. Int J Adv EnggTech.5(4),12-18. https://www.academia.edu/70486137/The_Benefits_and_Applications_of_Nanocomposites.
13. Bakis C. E., Bank L. C., ASCE F., Brown V. L., ASCE M., Cosenza E., Davalos J. F., ASCE A.M., Lesko J. J., Machida A., Rizkalla S. H., Asce F., Triantafillou T. C. and ASCE M. (2002). Fiber-reinforced polymer composites for construction-state-of-the-art review. Journal of Composites for Construction 73-87.<https://doi.org/10.1061/~ASCE11090-0268~2002!6:2~73!>
14. Charles Chikwendu Okpala. (2013). Nanocomposites An Overview, International Journal of Engineering Research and Development. 8 (11), 17-23. <http://www.ijerd.com/paper/vol8-issue11/C08111723.pdf>
15. Sachse S., Gendre L., Silva F, Zhu H., Leszczyńska A., Pielichowski K; Ermini V. and Njuguna J. (2013). On Nanoparticles Release from Polymer Nanocomposites for applications in Lightweight Automotive Components“, Journal of Physics: Conference Series, 429, 012046. Available at: <https://doi.org/10.1088/1742-6596/429/1/012046>.
16. Hurang Hua; Landon Onyebuekea and Ayo Abatanb. (2010). Characterizing and Modeling Mechanical Properties of Nanocomposites, Review and Evaluation. Journal of Minerals & Materials Characterization& Engineering, 9 (4), 275-319.<https://doi.org/10.4236/jmmce.2010.94022>.
17. Shehata F., Abdelhameed M., Fathy A., Elmahdy M. (2011). Preparation and Characteristics of cu-Al₂O₃ Nanocomposite, OJMetal, 1, 25-33.<https://doi.org/10.4236/ojmetal.2011.12004>.
18. Shokuhfar A; Öchsner Andreas; Shokuhfar Ali .(2013). New frontier of nanoparticles and nanocomposite materials, Novel principles and techniques. Advanced, structured materials,4(4), 500 .<https://link.springer.com/book/10.1007/978-3-642-14697-8>.
19. Mrazova .M. (2013). Advanced composite materials of the future in aerospace industry. Incas Bulletin. 5,(3) pp. 139 – 150: <https://doi.org/10.13111/2066-8201.2013.5.3.14>.
20. Basati F. , M.H.Yas. (2023). Dynamic and Buckling Analysis of Hybrid Composite BeamStrengthened with Carbon Fibers/Aramid Fibers under Temperature Gradient. Mechanics of Advanced Composite Structures. 11. 203–216.<https://doi.org/10.22075/mac.2023.29813.1475>.
21. Emrah Madenci, Yasin Onuralp Özkılıç , Ceyhun Aksoylu, Muhammad Rizal Muhammad Asyraf, Agusril Syamsir, Abu Bakar Mohd Supian and Nicolay Mamaev. (2023). Buckling Analysis of CNT-Reinforced Polymer Composite Beam Using Experimental and Analytical Methods. Materials, 16, 614.<https://doi.org/10.3390/ma16020614>.

22. Ansari R., Hemmatnezhad. M. (2013). Nonlinear finite element vibration analysis of double-walled carbon nanotubes based on Timoshenko beam theory. *Journal of Vibration and Control*. 19,75-85. Available at: <https://doi.org/10.1177/1077546311429838>.
23. NeclaTogun and Süleyman Murat Bagdatli. (2016). Nonlinear Vibration of a Nanobeam on a Pasternak Elastic Foundation Based on Non-Local Euler-Bernoulli Beam Theory. *Math. Comput. Appl.*, 21 (3), 1-19. <https://doi.org/10.3390/mca21010003>.
24. Rakrak Kaddour, Zidour Mohamed , Heireche Houari, Bousahla Abdelmoumen Anis and Chemi Awda. (2016). Free vibration analysis of chiral double-walled carbon nanotube using non-local elasticity theory. *Advances in Nano Research, An Int'l Journal* 4 (1); 31-44. <https://doi.org/10.12989/anr.2016.4.1.031>.
25. Hajnayeb. Ali and Khadem S.E. (2015). An analytical study on the nonlinear vibration of a doublewalled carbon nanotube. *Structural Engineering and Mechanics, An Int'l Journal*. 54 (5), 987-998. <https://doi.org/10.12989/sem.2015.54.5.987>.
26. Gafour. Y., Mohamed Zidour, Abdelouahed Tounsi, Houari Heireche and Abdelwahed Semmah. (2013). Sound wave propagation in zigzag double-walled carbon nanotubes embedded in an elastic medium using nonlocal elasticity theory. *Physica E: Low-dimensional Systems and Nanostructures*, 48, 118-123. <https://doi.org/10.1016/j.physe.2012.11.006>.
27. Danilo Karličić, Predrag Kozić and Ratko Pavlović. (2015). Flexural vibration and buckling analysis of single-walled carbon nanotubes using different gradient elasticity theories based on reddy and huu-tai formulations. *Journal of theoretical and applied mechanics*. 53, (1), 217-233. <https://doi.org/10.15632/jtam-pl.53.1.217>.
28. Ramezani Hossein Ali Akbari, Roohollah Dehghani and Firouz Abadi. (2015). Nonlinear Free Vibration of Single-Walled Carbon Nanotubes Embedded in Viscoelastic Medium Based on Asymptotic Perturbation Method”, *Journal of Science and Engineering*; 6 (02), 42-58. www.oricpub.com.
29. Soltani P., Bahramian R. and Saberian J. (2015). Nonlinear Vibration Analysis of the Fluid-Filled Single Walled Carbon Nanotube with the Shell Model Based on the Nonlocal Elasticity Theory. *Journal of Solid Mechanics*, 7 (1) 58-70; [Dor. 20.1001.1.20083505.2015.7.1.5.6](https://doi.org/10.1001/1.20083505.2015.7.1.5.6)
30. Tuan Ngoc Nguyen, Kim Nam-Il and Jaehong Lee. (2017). Static behavior of nonlocal Euler-Bernoulli beam model embedded in an elastic medium using mixed finite element formulation. *Structural Engineering and Mechanics, An Int'l Journal*, 63 (2),137-146. <https://doi.org/10.12989/sem.2017.63.2.137>.
31. Dihaj Ahmed, Mohamed zidour, Mustapha Meradjah, Kaddour Rakrak, Houari Heireche. (2018). Free vibration analysis of chiral double-walled carbon nanotube embedded in an elastic medium using non-local elasticity theory and Euler Bernoulli beam model. *Structural Engineering and Mechanics, An Int'l Journal* 65 (3),335-342. <https://doi.org/10.12989/sem.2018.65.3.335>.
32. Hamidi A, Zidour M, Bouakkaz K., Bensattalah T. (2018). Thermal and Small-Scale Effects on Vibration of Embedded Armchair Single-Walled Carbon Nanotubes. *Journal of Nano Research* 51, 24-38. <https://doi.org/10.4028/www.scientific.net/JNanoR.51.24>.
33. Iijima, S.; Brabec, C.; Maiti, A.; Bernholc, J. (1996). Structural flexibility of carbon nanotubes. *Chemical. Physics journal*. 104, 2089-2092; <https://doi.org/10.1063/1.470966>.
34. Motevalli B. Montazeri A.,Tavakoli-Darestani R. Rafii-Tabar H., (2012). Modeling the buckling behavior of carbon nanotubes under simultaneous combination of compressive and torsional loads, *Physica E: Low-dimensional Systems and Nanostructures*, Volume 46, Pages 139-148. <https://doi.org/10.1016/j.physe.2012.09.006>.
35. Ball, P., Roll Up for the Revolution. (2001). *Nature*. Nov 8; 414 (6860):142-4. <https://doi.org/10.1038/35102721>.

36. Qian, D., Wagner, G. J., Liu, W. K., Yu, M. F., and Ruoff, R. S. 2002. Mechanics of Carbon Nanotubes. *Applied Mechanics Reviews.*, 55 (6), 495–533. <https://doi.org/10.1115/1.1490129>.
37. Zhang, C. L., and Shen, H. S. 2007. Buckling and Postbuckling of Single-Walled Carbon Nanotubes Under Combined Axial Compression and Torsion in Thermal Environments. *Physical Review B*, 75, 045408. <https://doi.org/10.1103/PhysRevB.75.045408>.
38. Chemi A, Zidour M., Heireche H., Rakrak K., Bousahla AA. (2018). Critical Buckling Load of Chiral Double-Walled Carbon Nanotubes Embedded in an Elastic Medium. *Mechanics of Composite Materials* 53 (6), 827-836. <https://doi.org/10.1007/s11029-018-9708-x>
39. Mahmood M. Shokrieh, Akbar Hasani, Larry B. Lessard. (2004). Shear buckling of a composite drive shaft under torsion, *Composite Structures*, Volume 64, Issue 1, 63-69. [https://doi.org/10.1016/S0263-8223\(03\)00214-9](https://doi.org/10.1016/S0263-8223(03)00214-9).
40. Wang X Guoxing Lu, Y.J. Lu. (2006). Buckling of embedded multi-walled carbon nanotubes under combined torsion and axial loading, *International Journal of Solids and Structures*, V 44, Issue 1, 336-351: <https://doi.org/10.1016/j.ijsolstr.2006.04.031>.
41. Hiroyuki Shima. Buckling of Carbon Nanotubes. A State of the Art Review. Open Access submitted to *Materials*. <https://doi.org/10.3390/ma5010047>.
42. Zhang, Y. Y.; Wang, C. M.; Tan, V. B. C. 2007. Buckling of Carbon Nanotubes: A Literature Survey TY - JOUR. *Journal of Nanoscience and Nanotechnology*, Vol. 7, no 12, pp. 4221-4247(27): <https://doi.org/10.1166/jnn.2007.924>.
43. Chang, Tienchong, Guo, Wanlin, Guo, X.M. (2005). Buckling of multiwalled carbon nanotubes under axial compression and bending via a molecular mechanics model. *Phys. Rev. B*. 72. <https://doi.org/10.1103/PhysRevB.72.064101>.
44. Patryk Rozylo, Michal Rogala and Jakub Pasnik. (2023). Buckling Analysis of Thin-Walled Composite Structures with Rectangular Cross-Sections under Compressive Load. *Materials* 2023, 16, 6835. <https://doi.org/10.3390/ma16216835>
45. Kuba Rosłaniec, Patryk Różyło, Michał Kuciej. (2023). Buckling of Compressed Thin-Walled Composite Structures with Closed Sections. *Advances in Science and Technology Research Journal*, 17(6), 63–72. <https://doi.org/10.12913/22998624/174193>
46. Belmahi Samir, M Zidour, M Meradjah, T Bensattalah. (2018) .Analysis of boundary conditions effects on vibration of nanobeam in a polymeric matrix. *Structural Engineering and Mechanics*, An.Int'l.Journal, V67-5-517-525. <https://doi.org/10.12989/sem.2018.67.5.517>
47. Dobromir Dinev. (2012). Analytical solution of beam on elastic foundation by singularity functions, *Engineering MECHANICS*, Vol. 19, No. 6, p. 381–392.
48. Bao WenXing a,b,, Zhu ChangChuna , Cui WanZhao a .(2004). Simulation of Young’s modulus of single-walled carbon nanotubes by molecular dynamics. *Physica B* 352. 156–163. <https://doi.org/10.1016/j.physb.2004.07.005>.

Notes on Contributors

Doctor Belmahi Samir, Lecturer (research professor) since 2013, University Centre of Maghnia, Algeria, research area: composite materials and concrete, reinforcement of structures.....

Doctoral student Nedjm Eddine Boulesnane, University of Tiaret Algeria, research area: composite materials and concrete, reinforcement of structures....

Professor Zidour Mohamed (research professor) since 2011, University of Tiaret Algeria, research area: composite materials and concrete, reinforcement of structures....

ORCID

Belmahi Samir, <http://orcid.org/0000-0001-4824-2143>

Boulesnane Nedjm Eddine , <http://orcid.org/0009-0005-7334-7990>

Zidour Mohamed, <https://orcid.org/0000-0002-0189-4523>